

# On the adiabatic walking of plasma waves in a pulsar magnetosphere

George I. Melikidze<sup>1,2</sup>

Dipanjan Mitra<sup>3</sup>

Janusz Gil<sup>1</sup>

<sup>1</sup>*Kepler Institute of Astronomy, University of Zielona Gora, Lubuska 2, 65-265 Zielona Góra, Poland*

<sup>2</sup>*Abastumani Astrophysical Observatory, Ilia State University, 3-5 Cholokashvili Ave., Tbilisi, 0160, Georgia*

<sup>3</sup>*National Centre for Radio Astrophysics Ganeshkhind, Pune 411 007 India*

`gogi@astro.ia.uz.zgora.pl`

`dmitra@ncra.tifr.res.in`

`jag@astro.ia.uz.zgora.pl`

## ABSTRACT

The pulsar radio emission is generated in the near magnetosphere of the neutron star and it has to propagate through the rest of it to emerge into the interstellar medium. An important issue is whether this propagation affects the planes of polarization of the generated radiation. Observationally, there is a sufficient evidence that the emerging radiation is polarized parallel or perpendicular to the magnetic field line planes that should be associated with the ordinary O and extraordinary X plasma modes respectively, excited by some radiative process. This strongly suggests that the excited X- and O-modes are not affected by the so-called Adiabatic Walking that causes a slow rotation of polarization vectors. In this paper we demonstrate that the conditions for the Adiabatic Walking are not fulfilled within the soliton model of pulsar radio emission, in which the coherent curvature radiation occurs at frequencies much lower than the characteristic plasma frequency. The X-mode propagates freely and observationally represents the primary polarization mode. The O-mode has difficulties in escaping from the pulsar plasma, nonetheless it is sporadically observed as a weaker secondary polarization mode. We discuss a possible scenario under which the O-mode can also escape from the plasma and reach an observer.

*Subject headings:* pulsars: general — radiation mechanisms: nonthermal

## 1. Introduction

The brightness temperature (exceeding  $10^{12}$  K by many orders of magnitude) deduced from the observed radio flux densities strongly implies that the pulsar radiation must be emitted coherently. Generally, the coherent pulsar radio emission can be generated by means of either a maser or a coherent curvature mechanism (e.g. Ginzburg & Zhelezniakov 1975; Ruderman & Sutherland 1975; Melikidze & Pataraya 1980, 1984; Kazbegi, Machabeli & Melikidze 1991; Melikidze, Gil & Pataraya 2000). There is general agreement that this radiation is emitted in strongly magnetized electron-positron plasma well inside the light cylinder. Many observational constraints on emission altitudes imply that the emitted radiation detaches from the ambient plasma at altitude  $r_d$  less than 10% of the light cylinder radius<sup>1</sup>  $R_{LC} = Pc/2\pi$  (e.g. Cordes 1978; Blaskiewicz, Cordes & Wasserman 1991; Rankin 1993; Kijak & Gil 1997; Mitra & Deshpande 1999; Gangadhara & Gupta 2003; Mitra & Li 2004; Krzeszowski et al. 2009). The emission is clearly emitted at a lower altitude  $r_{em}$  and it must propagate through the magnetosphere to reach an observer, that is  $r_{em} \leq r_d$ . The plasma properties in the region between  $r_{em}$  and  $r_d$  can, in principle, influence the nature of waves, and in Section 3.4 we will discuss propagation effects, especially those that concern the polarization state.

Once the waves are generated in the emission region ( $r \sim r_{em}$ ), then in the propagation region ( $r_{em} < r < r_d$ ) they naturally split into the ordinary O-mode and extraordinary X-mode, which correspond to the normal modes of wave propagation in the strongly magnetized plasma (see e.g. Arons & Barnard 1986; Lominadze et al. 1986). The ordinary waves are polarized in the plane of the wave vector  $\mathbf{k}$  and the local magnetic field  $\mathbf{B}$  and their electric field has a component along both  $\mathbf{k}$  and  $\mathbf{B}$ . Therefore, they interact strongly with plasma particles and thus encounter difficulty in escaping from the magnetosphere. On the other hand, the extraordinary waves are linearly polarized perpendicularly to  $\mathbf{k}$  and  $\mathbf{B}$ . As a result the X-mode can propagate through the magnetospheric plasma almost as in vacuum.

It is important to realize that there is also observational evidence confirming the extraordinary mode to be dominant in the pulsar radiation. Lai, Chernoff & Cordes (2001), based on the X-ray image of the Vela pulsar wind nebula were able to model the pulsars rotation axis as it is projected in the sky. The X-ray image showed two X-ray arcs that were interpreted to be a result of outflowing relativistic particles from two diametrically opposite pulsar beams interacting with the environment around the pulsar. The bisection of the two arcs gave the direction of the rotation axis projected on the sky plane. Further they used the radio polarization property of the Vela pulsar where the linear polarization position angle

---

<sup>1</sup>Let us note that this may not be true for the millisecond pulsars.

traverse is well represented by the so called rotating vector model (RVM). In this model the polarization position angle (PPA) of the linear polarization executes a s-shaped track across the pulses. This was interpreted by Radhakrishnan & Cooke (1969) as electric field vector associated with the range of open dipolar magnetic field planes intersected by the observer’s line of sight. The steepest gradient (SG) point in the PPA track is usually considered as the fiducial point located in the plane containing the magnetic dipole and the rotation axis (at least in slow pulsars). Lai, Chernoff & Cordes (2001) used the value of the absolute PPA at the SG point ( $PA_{\circ}$ ), and found its direction to be perpendicular to the rotation axis, which means that the electric vector emanating out of the Vela pulsar is orthogonal to the dipolar magnetic field line planes. Hence it was the extraordinary (X) mode (Lai, Chernoff & Cordes 2001). This is a very significant observational result, as for the first time it was possible to verify that the electric field vectors emerging from the Vela pulsar magnetosphere are perpendicular to the dipolar magnetic field line planes. The Vela X-ray observations also showed that the proper motion direction ( $PM_v$ ) of the pulsar is aligned with the rotation axis.

An X-ray pulsar wind nebula is not observed for majority of the pulsars, and hence the direction of the rotation axis on the plane of the sky cannot be determined directly. However, based on several careful recent studies by Johnston et al. (2005), Rankin (2007), and Noutsos et al. (2012, 2013), a bimodal distribution of  $\Psi=(PM_v - PA_{\circ})$  centered around  $0^{\circ}$  and  $90^{\circ}$  has been observed. Mitra, Rankin & Gupta (2007) used this distribution, along with the assumption that the pulsar spin axis is aligned with the proper motion direction to establish the direction of the emerging wave at  $PA_{\circ}$  with respect to the magnetic field line planes.

It is instructive to follow and generalize their arguments. The proper motion measurement of many pulsars can give the projected orientation of the rotation axis with respect to the celestial north. We can also independently measure the absolute position angle  $PA_{\circ}$  (corrected for all instrumental and propagation effects) at the fiducial point (SG point and/or profile midpoint). Then we can find the difference  $\Psi$  between these angles, and amazingly  $\Psi$  shows a bimodal distribution centered around  $0^{\circ}$  and  $90^{\circ}$ . Let us ask the question how this can happen? It is possible only if the spin axis is either parallel or perpendicular to the direction of the proper motion and at the same time the  $PA_{\circ}$  coincides either with the fiducial plane or the plane perpendicular to it. Let us assume for the moment that  $PA_{\circ}$  is at some arbitrary angle with respect to the fiducial plane. Then we have to find such a direction for the velocity vector which is either perpendicular or parallel to the polarization vector at the fiducial point. Then this needs to be extended to all pulsars in the sample, in which every pulsar could have different  $PM_v$  and  $PA_{\circ}$ . Such fine tuning is very difficult, given that  $PM_v$  and  $PA_{\circ}$  are determined by two completely independent phenomena.

Hence, the most likely explanation is that the velocity vector should be either parallel or perpendicular to the rotation axis and/or  $PA_{\circ}$  should be parallel or perpendicular to the fiducial plane. The latter is a natural consequence of pulsar radio emission being excited by the soliton coherent curvature radiation, as argued by Melikidze, Gil & Pataraya (2000), Gil, Lyubarsky & Melikidze (2004), and Mitra, Gil & Melikidze (2009), hereafter Papers I, II, and III, respectively. As for the former possibility, it is yet to be established by the supernova explosion theory (e.g. Tademaru & Harrison 1975; Cowsik 1998; Spruit & Phinney 1998). However, in three cases for which X-ray information is available (Vela, B0656+14 and J0538+2817; see Rankin 2007), the rotation axis is parallel to the proper motion direction. If this can be generalized in the future, then the pulsars with  $\Psi \sim 90^{\circ}$  in the bimodal distribution of  $\Psi$  (see Figure 3 in Rankin 2007) represent the X-mode observed as the primary polarization mode (PPM). Similarly those with  $\Psi \sim 0^{\circ}$  represent the O-mode observed as a secondary polarization mode (SPM).

Recently in Paper III the authors showcased highly polarized subpulses from single pulses for a number of pulsars, in which the position angle of the linear polarization closely followed the mean position angle traverse. They further conjectured that the observed polarization state of some subpulses represents the extraordinary mode excited by the soliton coherent curvature radiation. This conclusion was conditional on non fulfilment of the so called Adiabatic Walking Condition (AWC henceforth) first introduced by Cheng & Ruderman (1979, CR79 hereafter). The conclusions of Paper III can remain unnoticed, since it lacked strong and convincing arguments that the polarization direction of the generated waves cannot be changed by the adiabatic walking. In this paper we will give further arguments, both from observational and theoretical points of view, that the AWC is indeed not satisfied in pulsar magnetospheres, under conditions required for the soliton coherent curvature radiation emitted at frequencies much lower than the local characteristic plasma frequency. Thus the X-mode excited by the coherent curvature radiation can freely leave the pulsar and reach the observer. This mode represents the observationally dominant PPM. We will also present observational evidence for the O-mode, excited by the curvature radiation. This mode dominates at the emission region (about 6 times stronger than the X-mode)<sup>2</sup>, but it cannot freely propagate through magnetospheric plasma. We will discuss a possible scenario under which part of the O-mode can escape from the magnetosphere. This mode would then correspond to the weaker secondary polarization mode (SPM).

---

<sup>2</sup>This effect is well known for the vacuum case (e.g. Jackson 1975) and for the plasma environment it was generalized by Gil, Lyubarsky & Melikidze (2004); see the last paragraph in Section 5 of their paper.

## 2. Importance of the single-pulse polarization properties

In Figure 1 we show an example of the observed composite and single pulse polarization in pulsar PSR B2045–16<sup>3</sup> observed with the Giant Meterwave Radio Telescope (GMRT, see Paper III for observation details) near Pune, India. Two highly polarized subpulses, appearing in two different single pulses in the longitude range corresponding to the leading profile component are shown in the left panels of the figure. Their PPA traverses correspond to the two orthogonal polarization modes. These subpulses represent essentially single polarization modes close to 100% polarization each. They obviously do not suffer from any significant depolarization, and the PPA associated with the leading profile component follow the mean position angle traverse.

Without any further modeling we are unsure about the orientation of the polarization vectors of these modes with respect to the pulsar magnetic field line planes. We can however adopt the strategy taken by Mitra, Rankin & Gupta (2007), where they determine the direction of the modal PPAs with respect to the projected magnetic field line planes by comparing the fiducial PPA and proper-motion directions as explained in the introduction. The proper motion of this pulsar is  $PM_v=92^\circ \pm 2$  and the absolute value of PPA at the fiducial longitude  $PA_o=-3^\circ \pm 5$ , which gives the quantity  $\Psi = (PM_v - PA_o) = 95^\circ \pm 5$  (see Rankin 2007; Morris et al. 1979, 1981). Thus, based on the assumption that the pulsar proper motion is directed along the rotation axis<sup>4</sup>, the emerging electric field at the fiducial point of the dominant PPA mode is perpendicular to the dipolar magnetic field line plane. As seen in the right panel of Fig 1, the fiducial point is determined by the stronger PPM and hence this point should be associated with the perpendicular or extraordinary (X) mode. The weaker SPM should then be associated with the parallel or ordinary (O) mode. As it was pointed out in Paper II, this argument can be extended to the rest of the PPA traverse which follow the RVM model, and hence the polarization state for this pulsar at each pulse phase along the PPM represents the X-mode polarized perpendicularly to the magnetic field line planes.

As a summary of this section, let us consider a fictitious radiation mechanism that generates two orthogonal polarization modes without being parallel or perpendicular to the magnetic field line planes. To explain the observed polarization in Figure 1, one has to

---

<sup>3</sup> PSR B2045–16 is a slowly rotating pulsar with period of 1.9 sec, and its position angle curve suffers almost no distortions due to the effects of aberration and retardation (see Mitra & Li 2004, for a detailed discussion), and hence follow the RVM rather accurately.

<sup>4</sup>Recently Noutsos et al. (2012) performed a statistical analysis for 54 pulsars to test the pulsar rotation axis and proper motion alignment, and found strong evidence for this effect, excluding that these vectors are completely uncorrelated with > 99% confidence.

invoke a propagation effect that rotates the modes in such a way that they emerge almost purely polarized parallelly or perpendicularly to the dipolar magnetic field line planes. One of the such mechanisms was proposed by CR79, who introduced the so-called adiabatic walking scenario. They argued, that even chaotically oriented polarization directions will slowly rotate while the waves propagate away from the generation region. As a result within the polarization limiting region (beyond which the waves detach from the plasma; see e.g. Arons & Barnard 1986) all the chaotic polarizations will get arranged and thus the emerging polarization will consist of the two orthogonal modes.<sup>5</sup> However, this does not mean that they will be polarized parallel or perpendicular to the planes of dipolar magnetic field lines, as demonstrated in Figure 1 (a collection of such pulses is presented in Figure 2). This would require unrealistic fine tuning in every pulse longitude<sup>6</sup>. Therefore, based on our observations, we conclude that this radiation is not affected by the adiabatic walking and we receive the generated polarization pattern. The only radiation mechanism that can distinguish the magnetic field line planes is the curvature radiation excited in pulsar plasma (Paper II and III). In the next section we will demonstrate that the AWC is not satisfied in the pulsar plasma with characteristics allowing generation of the coherent soliton curvature radiation. Therefore the adiabatic walking does not affect the polarization of the plasma X- and O-waves excited by this radiation mechanism.

Before closing this section, it is important to comment on the majority of subpulses that has intermediate, low or undetectable polarization, where the PPA's do not necessarily follow the mean PPA traverse. This property is in general expected in the currently discussed coherent curvature radiation model (Papers I, II and III). The subpulse in this model results from incoherent addition of a large number of independently emitting solitons. Each of these solitons excite the X- and O-modes in the plasma, however the modes get separated (although, in this paper we will show that the modes do not change their state of polarization) and further the amplitude of the O-mode can be significantly damped. Before the modes emerge from the plasma, the incoherent addition of a large number of such waves (with random contribution of X- and O-modes both in amplitude and phase) leads to a range of observed depolarization values (detailed considerations of that scenario has been postponed to a separate paper). Only in certain occasions the plasma conditions are such that either the X- or O-mode emerges as the dominant radiation mode, which is observed as close to 100% polarized subpulse emission. In fact the highly polarized subpulses presented in this

---

<sup>5</sup>The polarization of one mode is parallel to the local  $\mathbf{k}$  and  $\mathbf{B}$  plane and the polarization of other mode is perpendicular to it. This local plane in general does not coincide with the plane of magnetic field lines.

<sup>6</sup>It is well known that the variations of the polarization position angle across the pulse window trace the range of dipolar magnetic field line planes as predicted by the RVM model.

paper and Paper III are indeed rare (typically  $< 1\%$ ) occurrences. However, they are very important to be studied as they can reveal the true nature of pure X- and O-modes.

### 3. Plasma waves in the near magnetosphere and Pulsar emission Mechanism

The coherent curvature radiation has been considered as a natural emission mechanism for the observed pulsar radiation (e.g. Ruderman & Sutherland 1975, RS75 hereafter; Benford & Buschauer 1983; Melikidze & Pataraya 1984), although several key issues in this theory remained unresolved for a long time. For example, the theory of formation of charged bunches leading to curvature radiation in a plasma was not developed. Also, it was not clear how the radiation emerges from the magnetospheric plasma. The recent attempts to build and develop a self consistent theory of curvature radiation for pulsar radio emission has been published in Papers I, II, and III. Under the framework of this theory, here we recapitulate the physical processes generating the magnetospheric plasma that leads to the observed pulsar coherent radio emission.

The basic requirement of this theory is the presence of non-stationary inner acceleration region above the polar cap. The prototype of this region was the inner vacuum gap suggested by RS75. The formation of their gap was based on the overestimated value, by at least an order of magnitude, of the binding energy of iron ions in the neutron star crust (Gil, Melikidze & Geppert 2003, and referencies therein). As a result the accelerating potential drop along the magnetic field in the gap was very high, exceeding  $10^{13}$  volts. In such high potential drop the backflowing particles heat the polar cap to enormous temperatures close to  $10^7$  K, which has been never observed in the form of intense thermal X-rays from polar caps. Also the so called subpulse drift would be too fast as compared with the observed drift rates (Gil, Melikidze & Geppert 2003, and referencies therein). Therefore the original RS75 model called for a revision from the very beginning.

In the mean time, new calculations of binding energy of iron ions was published by Jones (1986) and similar study was performed using different and more precise method by Medin & Lai (2006, 2007). These calculations demonstrated that the vacuum gap could be formed only if the actual surface magnetic field at the polar cap was close to  $10^{14}$  G, much higher than the dipolar magnetic field at the surface of most pulsars. To preserve the idea of the inner accelerator region one has to invoke a strong non-dipolar crust anchored surface field much stronger than the dipolar component at the surface. It appears that such surface magnetic fields are likely to be produced in the neutron star crust by Hall-drift instabilities (Geppert, Gil & Melikidze 2013, and references therein).

Based on these ideas Gil, Melikidze & Geppert (2003) proposed the Partially Screened Gap (PSG hereafter) model for the inner acceleration region. In this model the backflowing particles heating the polar cap cause a thermal outflow of iron ions, which partially screen the gap potential drop. The more they screen, the less the lower potential drop causes heating and therefore less screening at the same time. So the thermostatic regulation will occur establishing the surface temperature at a value close to but slightly below the so-called critical temperature (at which iron ions would be extracted at the co-rotation limited Goldreich-Julian charge density). In the consequence the maximum value of the potential drop will be about one order of magnitude lower as compared with the vacuum case of RS75. This potential drop is still high enough to drive the non-stationary sparking discharge in the PSG and produce the electron positron primary plasma similarly to that envisioned by RS75. The presence of an additional iron ion component does not influence significantly the production of the secondary plasma. The so-called multiplicity factor  $\kappa = n_{\pm}^s/n_{GJ}$  (where  $n_{\pm}^s$  is charge density of the secondary plasma and  $n_{GJ}$  is the Goldreich-Julian charge density) lies in the range  $100 \leq \kappa \leq 10^5$  (for details see Asseo & Melikidze (1998), also Szary (2013) for application to the PSG model). The structure of the secondary plasma is formed by the sparking discharge of the PSG.

### 3.1. Plasma Dispersion relation at the Radio Emission Region

Let us now consider the magnetospheric plasma waves in the radio emission region, i.e. the tube of the open field lines consisting of electron and positron of secondary plasma at altitudes  $r$  of about 50 to 100 stellar radii, where the coherent curvature radio emission is expected to originate. We start with the dispersion equation in the pulsar frame of reference assuming that  $\mathbf{k}$  is along the  $z$ -axis and  $\vartheta$  is the angle between the local magnetic field  $\mathbf{B}$  and the wave vector  $\mathbf{k}$  (see Kazbegi, Machabeli & Melikidze 1991, KMM91 hereafter). The distribution function of the secondary plasma is close to a gaussian distribution, centered at  $\gamma = \gamma_s \gg 1$ , having a spread of  $\Delta\gamma/\gamma_s \ll 1$  (Paper II, Szary 2013). At the altitudes  $r = (50 - 100) \times 10^6$  cm the fractional altitude  $\mathfrak{R} \equiv (r/R_{LC}) = 2\pi r/(cP)$  is for typical pulsars small ( $\mathfrak{R} = (0.01 - 0.1)P^{-1}$ ) and hence the ratio

$$\frac{\omega_p}{\omega_B} = 2.8 \times 10^{-4} \kappa^{0.5} P^{0.75} \dot{P}_{-15}^{-0.25} \mathfrak{R}^{1.5} \ll 1, \quad (1)$$

where  $\omega_p^2 = 4\pi e^2 \kappa n_{GJ}/m_e$  is the plasma frequency,  $\omega_B = eB/m_e c$  is the cyclotron frequency,  $m_e$ ,  $e$  and  $c$  correspond to the mass of the electron, charge of the electron and speed of light, respectively (in cgs units).

Using the conditions stated above we can neglect all terms containing  $\omega_B^{-1}$  and hence



the dispersion relation can be written in the form

$$\left(k^2 \frac{c^2}{\omega^2} - \varepsilon_{11}\right) E_1 - \varepsilon_{13} E_3 = 0, \quad (2)$$

$$\left(k^2 \frac{c^2}{\omega^2} - 1\right) E_2 = 0, \quad (3)$$

$$\varepsilon_{31} E_1 + \varepsilon_{33} E_3 = 0. \quad (4)$$

Here  $E_1$ ,  $E_2$  and  $E_3$  are the components of electric fields along  $x, y$  and  $z$  axes ( $y$ -axes is perpendicular to the plane of  $\mathbf{k}$  and  $\mathbf{B}$ ),  $\varepsilon_{11} = 1 - I \sin^2 \vartheta$ ,  $\varepsilon_{13} = \varepsilon_{31} = I \sin \vartheta \cos \vartheta$ ,  $\varepsilon_{12} = -\varepsilon_{21} = \varepsilon_{23} = -\varepsilon_{32} = 0$ ,  $\varepsilon_{33} = 1 - I \cos^2 \vartheta$ , where  $I$  can be expressed as:

$$I \equiv \frac{1}{2} \sum \omega_{p\alpha}^2 \int \frac{dp}{\gamma^3} \frac{f_\alpha}{(\omega - kv \cos \vartheta)^2}, \quad (5)$$

$\alpha$  denotes sum over electrons and positrons,  $\omega_p^2 = 4\pi e^2 n_\pm^s / m_e$ ,  $p$  and  $v$  are the dimensionless momentum and velocity of the particles along the magnetic field (see KMM91). Solving the above equations, we get the dispersion relation

$$1 - \frac{\omega^2}{k^2 c^2} = 0 \quad (6)$$

for the X-mode, which is linearly polarized along  $y$ -axes, while for the O-mode (polarized in  $xz$ -plane) the dispersion curve is a solution of the following equation

$$\frac{1}{2} \left(1 - \frac{k^2 c^2}{\omega^2} \cos^2 \vartheta\right) \sum \omega_{p\alpha}^2 \int \frac{dp}{\gamma^3} \frac{f_\alpha}{(\omega - kv \cos \vartheta)^2} = 1 - \frac{k^2 c^2}{\omega^2}. \quad (7)$$

Let us note, that under the condition (1) we can assume that the distribution functions for both electrons and positrons are identical. The difference between these functions is important for the soliton coherent curvature radiation as the slowly varying charge-density is proportional to  $\Sigma e_\alpha \omega_{p\alpha}^2$  and vanishes if the distribution functions are identical (see Equation (A19) in Paper I). On the other hand, those components of the linear permittivity tensor, i.e.  $\varepsilon_{12}$ ,  $\varepsilon_{21}$ ,  $\varepsilon_{23}$  and  $\varepsilon_{32}$ , which have non-zero value in the case of non-identical distribution functions (see, e.g. KMM91), are proportional to  $\omega_B^{-1}$  and are negligibly small (see Equation (1)). Thus, taking into account  $\Delta\gamma/\gamma_s \ll 1$  the distribution functions can be described by the delta-function at  $\gamma_s$  i.e.  $f_\pm \sim \delta(p - p_s)$ . For the purpose of our discussion this is a very reasonable assumption, as we are interested in the average features of the plasma, as for the peculiarities of plasma distribution they are irrelevant. Then, using  $v \approx 1 - 0.5\gamma^{-2}$  Equation (7) can be reduced to the following form:

$$1 - \frac{k^2 c^2}{\omega^2} = \frac{\omega_p^2}{\gamma_s^3} \frac{\left(1 - \frac{k^2 c^2}{\omega^2} \cos^2 \vartheta\right)}{\left(\omega - k \left(1 - \frac{1}{2\gamma_s^2}\right) \cos \vartheta\right)^2}, \quad (8)$$

where  $\gamma_s = (1 + p_s^2)^{0.5}$ . Equation (8) describes the ordinary modes (i.e. modes polarized in the plane of  $\mathbf{k}$  and  $\mathbf{B}$ ) of the magnetized electron-positron plasma and has two possible solutions, which correspond to two branches: O-mode and L-mode. In the conditions under consideration (see Section 3.2 for details), i.e.  $\vartheta \ll 1$  and  $\omega$  being in the range from 0 up to values that does not exceed  $\omega_0$  significantly (see Equation (9) below), the waves have following features: the L-mode is almost longitudinal, while the O-mode is almost transverse. Equation 8 cannot be solved analytically, and to demonstrate its basic properties the schematic representation of solutions are shown in Figure 3. In the frequency region  $\omega \gg \omega_0$  the polarization characteristics of the L- and O-modes change, the L-mode becomes almost electromagnetic while the O-mode turns to be almost longitudinal and as a subluminal wave, it undergoes strong Landau damping (see Section 3.5).

If  $\vartheta = 0$  (propagation along the local magnetic field direction) Equation (7) has two independent solutions. The purely transverse solution coincides with X-mode, while L-mode coincides with the purely longitudinal Langmuir wave, the dispersion equation of which is obtained by dividing Equation (7) by Equation (6). Two values of wave frequency can be distinguished. The first point is defined by  $k = 0$  for which the corresponding frequency is  $\omega = \omega_1 = \gamma_s^{-1.5}\omega_p$ . The second point is defined by the condition  $\omega = kc$ , i.e. the phase velocity equals  $c$  for which the corresponding frequency is

$$\omega = \omega_0 = 2\sqrt{\gamma_s}\omega_p. \quad (9)$$

In this paper we use the term characteristic frequency for  $\omega_0$ . It is important to note that Langmuir waves cannot be excited if  $\omega_1 < \omega < \omega_0$ , since the phase velocity exceeds the speed of light (superluminal waves). On the other hand, in frequency region  $\omega > \omega_0$  the phase velocity is less than the speed of light (subluminal waves), thus the two-stream instability can develop, provided that the plasma distribution function has a proper shape (see Asseo & Melikidze 1998; Lominadze et al. 1986, for details).

### 3.2. Domain of plasma parameters

Let us overview basic parameters of the secondary plasma flowing along the tube of open field lines in the observer's frame of reference. We will represent them in terms of the basic pulsar parameters  $P$  (in sec) and  $\dot{P} = \dot{P}_{-15} \times 10^{-15}$  (s/s), and as a function of the fractional altitude  $\mathfrak{R} = r/R_{LC}$  (see previous section). The cyclotron frequency  $\nu_B$  in the local magnetic field  $B$  can be expressed in GHz as,

$$\nu_B = \frac{\omega_B}{2\pi\gamma_s} = 5.2 \times 10^{-2} \frac{1}{\gamma_s} \left( \frac{\dot{P}_{-15}}{P^5} \right)^{0.5} \mathfrak{R}^{-3}. \quad (10)$$

The characteristic plasma frequency  $\nu_o$  in GHz can be written as:

$$\nu_o = \frac{\omega_0}{2\pi} = 2 \times 10^{-5} \kappa^{0.5} \sqrt{\gamma_s} \left( \frac{\dot{P}_{-15}}{P^7} \right)^{0.25} \mathfrak{R}^{-1.5}, \quad (11)$$

with  $\omega_0$  given by Equation (9). As the third parameter we present the characteristic frequency of the soliton curvature coherent radiation, which corresponds to the maximum of the power spectrum  $\nu_{cr}$  (see Figure 2 in Paper II),

$$\nu_{cr} = 1.2 \frac{c\Gamma^3}{2\pi\rho} = 0.8 \times 10^{-9} \frac{\Gamma^3}{P} \mathfrak{R}^{-0.5}, \quad (12)$$

where  $\rho$  is the radius of curvature of the dipolar magnetic field lines and  $\Gamma$  is the Lorentz factor of the emitting soliton, for which the opening angle of the radiation cone  $\vartheta \sim \Gamma^{-1}$ .

Figure 4 summarizes these basic plasma parameters for a canonical pulsar with  $P=1$  sec and  $\dot{P}_{-15}=1$ , in the observer's frame of reference as a function of fraction of the light cylinder distance, put into the context of the observed pulsar radio emission. The abscissa axis originates at the altitude of about 5 stellar radii, above which the crucial two stream instability can develop (Asseo & Melikidze 1998)<sup>7</sup>. The uppermost red line represents the cyclotron frequency  $\nu_B$  (given by Equation (10)), where  $\gamma_s = 200$  was chosen as an average Lorentz factor of the secondary plasma (note that in the scale used in this plot, changing  $\gamma_s$  between 100 to 1000 will not move noticeably the red line). This line demonstrates that any radiation with frequency higher than  $\nu_B$  will be damped by means of cyclotron resonance. The next pair of green lines represent the plasma frequency  $\nu_o$  (given by Equation (11)) calculated for  $\gamma_s = 200$  and two limiting values of  $\kappa = 100$  and  $10^4$ . Two grey lines parallel to the x-axis, represent the canonical range of the observed pulsar radio emission (between 30 MHz to 30 GHz), with a dashed line corresponding to 1 GHz. The remaining two dark blue lines represent characteristic frequencies  $\nu_{cr}$  of the curvature radiation (given by Equation (12)) calculated for the radius of curvature of dipolar field lines ( $\rho \sim 10^8$  cm) and for two values of the Lorentz factor of the charged soliton  $\Gamma = 600$  for the upper solid line and  $\Gamma = 400$  for the lower dashed line (see Paper II for details).

We can now briefly discuss how Figure 4 will alter for different pulsar periods. The frequencies  $\nu_o$  and  $\nu_B$  are much more sensitive to changing  $P$  than the characteristic frequency

---

<sup>7</sup>If in Equation (63) by Asseo & Melikidze (1998) we assume reasonably low values for the average Lorentz factor of plasma particles  $\gamma_p/10^2 \sim (0.5 - 0.7)$  and for the half-width of a plasma cloud  $\Delta\Psi/(5 \times 10^4) \sim (0.2 - 0.4)$  we find that a corresponding distance from the center of the star  $r$  ranges from a few to several stellar radii. Thus the altitude of about 5 stellar radii seems to be quite a good approximation for the minimal altitude at which the two-stream instability can develop.

of the curvature emission  $\nu_{\text{cr}}$ , which depends on period in the same way as the fractional distance. Therefore, the soliton curvature radiation can always develop in the proper region of altitudes. i.e about 50-100 stellar radii, irrespective of the value of  $P$ .<sup>8</sup>

Figure 4 corresponds to the total power and contains no information about the polarization properties of the observed radiation. These properties will be considered in Section (3.4) in the context of possible propagation effects.

### 3.3. The mechanism of coherent radio emission

Let us now briefly review the spark-associated soliton model of the coherent curvature radiation from pulsars (for details see Paper I and references therein). Like any plasma model for pulsar radiation this model is also based on development of some plasma instabilities. The only plasma instability that can arise at altitudes lower than 10% of the light cylinder is the two-stream instability (Lominadze et al. 1986; KMM91; Asseo & Melikidze 1998), as all other instabilities are suspended by the strong magnetic field. The two-stream instability is a result of the effective energy exchange between particles and waves, that can occur if the phase velocity of waves ( $\omega/k$ ) is near to the velocity of resonant particles ( $v_r$ ), i.e. the resonant condition  $(\omega - kv_r) = 0$  is satisfied. As it has been already mentioned, the resonance is possible in frequency region  $\omega > \omega_0$ . However, one should realize that amplification of waves occurs only if there is an excess of particles with velocities larger than the phase velocity of waves near the resonant point. In the opposite situation the waves will be damped (the Landau damping). Thus, the plasma distribution function should have a proper shape (e.g. Asseo & Melikidze 1998) for a two-stream instability development. Such conditions can naturally be realized if a plasma is produced via non-stationary gap discharge. The spark discharge timescale in the PSG is a few tens of microseconds and this results in overlapping of successive clouds of outflowing secondary plasma. Each elementary spark-associated plasma cloud has a spread in momentum and the overlapping of particles with different momentum leads to two stream instability in the secondary plasma cloud (RS75; Usov 1987; Asseo & Melikidze 1998). This triggers strong Langmuir turbulence in the plasma and if this turbulence is strong enough, the waves become modulationally unstable. The unstable wave packet described by the nonlinear Schrödinger equation leads to formation

---

<sup>8</sup>However for very long periods the available potential drop could not be high enough to power the primary beam, which leads to "death" of radio pulsars. It is also worth mentioning, that for very old pulsars the crustal strong surface field may not be supported by the Hall drift instability. Absence of the crustal field leads to switching off the creation of dense electron-positron plasma, necessary for a mechanism of the coherent pulsar radio emission (Geppert, Gil & Melikidze 2013).

of a quasi-stable nonlinear solitary wave, i.e. a soliton (Pataraya & Melikidze 1980). The longitudinal (along  $\mathbf{k}$ ) size of the soliton should be much larger than the wavelength of the linear Langmuir wave. Also it has to be charged to be able to radiate coherent curvature emission. Thus, the soliton bunch has to be charge separated, which can be caused either by difference in the distribution function of electrons and positrons, or by admixture of iron ions in the secondary plasma or by both these effects. A sufficient number of charged solitons is formed which can account for the observed radio luminosity in pulsars (Paper I). The wavelength of the emitted waves should be longer than the longitudinal size of the soliton  $\Delta$ . This is the necessary condition for the coherency of a curvature radiation process. Thus, the frequencies plotted in Figure (4) should obey the following constraints

$$\nu_{\text{cr}} < \frac{c}{\Delta} \ll \nu_o \ll \nu_B. \quad (13)$$

It is clearly seen from Figure (4) that the observed pulsar radiation cannot be generated at altitudes exceeding 10% of the light cylinder radius (practically the radio emission region should be contained between one to several percent of  $R_{LC}$ ; see dashed area in Figure (4)). This conclusion is based purely on the properties of plasma and the emission mechanism. And it corresponds perfectly to the other limits on emission heights obtained from observations and geometrical considerations (e.g. Cordes 1978; Blaskiewicz, Cordes & Wasserman 1991; Rankin 1993; Kijak & Gil 1997; Mitra & Deshpande 1999; Gangadhara & Gupta 2003; Mitra & Li 2004; Krzeszowski et al. 2009).

### 3.4. Adiabatic walking condition

While studying rotation of polarization planes of X- and O-modes propagating in the pulsar magnetospheric plasma CR79 introduced the AWC in the form of

$$\left| \frac{1}{k} \frac{\partial}{\partial x} \phi \right| \ll |\Delta N|, \quad (14)$$

where  $\Delta N$  is a change of  $N$  occurring during propagation of waves,  $\phi$  is the linear polarization angle (dimensionless) of the mode or some similar dimensionless parameter, which defines the mode polarization and  $1/k \equiv 2\pi\lambda$ , where  $\lambda$  is the wavelength<sup>9</sup>. Here  $N = N^{(o)} - N^{(x)}$  is the difference between refractive indices of O- and X-mode:

$$N^o = \frac{kc}{\omega}|_{\text{O-mode}} \text{ and } N^x = \frac{kc}{\omega}|_{\text{X-mode}}.$$

---

<sup>9</sup>This is the sufficient condition of CR79 (their Eq. 2). The necessary (adiabatic) condition of CR79 (their Equation (1)) is always satisfied, if plasma properties vary slowly enough.

Remembering that the polarization vector of waves is either tangent or normal to  $\mathbf{k}$  and  $\mathbf{B}$  plane, for a change of the dimensionless parameter  $\phi$  we can choose  $\Delta\phi = \Delta\vartheta/\vartheta$ , where  $\vartheta \sim 1/\Gamma$ . It expresses the fact that the change of angle  $\vartheta$  between  $\mathbf{k}$  and  $\mathbf{B}$  during propagation causes a corresponding change of the polarization vector. Thus, the polarization plane of a wave would rotate by the angle about unity ( $\Delta\phi \sim 1$ ) while it propagates the distance  $\Delta l = \Delta\vartheta\rho$ , if the AWC was fulfilled (see also Paper II).

In our formalism, as seen in Equation (6), the refractive index  $N^{(x)} = 1$  for all values of  $k$ . To obtain  $N^{(o)}$  we need to solve Equation (8), which, however, cannot be achieved analytically. But we can make following very reasonable assumption:

$$\frac{k^2 c^2}{\omega_{\circ}^2} \sin^2 \vartheta \ll 1 \quad (15)$$

This condition is consistent with Equation (13), which assumes that in the radio emission region the frequency of emitted waves ( $\nu_{\text{cr}} = kc/2\pi$ ) should be less than  $\nu_{\circ} = \omega_{\circ}/2\pi$ . As  $\sin \vartheta$  cannot exceed unity, the above condition is always valid for emitted waves. The solution of Equation (8) for the O-mode under the condition expressed above is

$$\omega = kc \cos \vartheta \left( 1 - \frac{1}{2} \frac{k^2 c^2}{\omega_{\circ}^2} \sin^2 \vartheta \right). \quad (16)$$

Thus it is straightforward to show that

$$N^{(o)} = \frac{kc}{\omega} \Big|_{\text{O-mode}} = \cos^{-1} \vartheta \left( 1 + \frac{k^2 c^2}{2\omega_{\circ}^2} \sin^2 \vartheta \right). \quad (17)$$

Then assuming  $\vartheta \ll 1$ , which is very reasonable assumption for the relativistic plasma, we obtain that

$$N = N^{(o)} - 1 = \frac{1}{2} \vartheta^2 \left( 1 + \frac{k^2 c^2}{\omega_{\circ}^2} \right). \quad (18)$$

In order to examine validity of the AWC we can use  $|\partial\phi/\partial x| \approx |\Delta\phi/\Delta l| = 1/\vartheta\rho$  and  $|\Delta N| = |\vartheta\Delta\vartheta|$ , therefore the AWC can be rewritten in the following form

$$\vartheta^3 \left( \frac{\Delta\vartheta}{\vartheta} \right) \gg \frac{1}{\rho} \frac{\rho}{\Gamma^3}. \quad (19)$$

Let us note that  $\Delta\vartheta/\vartheta \sim 1$  (meaning that AWC is fulfilled) only if  $\vartheta^3 \gg \Gamma^{-3}$ . However,  $\vartheta \approx \Gamma^{-1}$ , thus we can safely conclude that the AWC is not satisfied under our assumptions. Therefore, the adiabatic walking cannot affect the polarization of waves excited by the soliton curvature radiation.

It may be interesting to figure out why we have found just an opposite conclusion to that obtained by CR79. The main difference comes from the condition  $k^2 c^2 = \omega^2 \ll \omega_{\circ}^2$

which must be satisfied in the case of soliton curvature radiation (Paper I). In the case of the classical curvature radiation model of RS75 that was used by CR79 the characteristic frequencies should obey the following condition  $k^2 c^2 = \omega^2 \approx \omega_o^2$  (since their bunches are formed by linear Langmuir waves).

In the frequency range  $\omega \sim \omega_o$  (which is not allowed in the soliton mechanism, Paper I) the dispersion curve of the O-mode deviates significantly from the X-mode dispersion line  $\omega = kc$ , as compared with the frequency range of soliton curvature emission  $\omega \ll \omega_o$  (marked by the shadowed area in Figure 4). It is difficult to demonstrate these differences in Figure 3 and therefore we present the numerical solution for  $|N|$  in Figure 5, obtained for three values of  $\vartheta$ . These figures are equivalent to each other since Figure 5 represents simply the difference between the O-mode and the X-mode in Figure 3. As we can see from Figure 5, below  $kc/\omega_o \sim 0.1$ ,  $|N|$  stays unchanged, so  $\Delta N \sim 0$  and the AWC cannot be satisfied. This is the range of soliton coherent curvature radiation considered in this paper as the viable pulsar radio emission mechanism. Beyond this range  $|N|$  becomes varying so  $\Delta N$  can attain relatively large values and therefore the AWC can be satisfied. This range was considered by CR79 who used RS75 radiation model, in which charged bunches formed by linear Langmuir waves emitted coherent curvature radiation. However this radiation mechanism should not be realized physically as argued for the first time by (Lominadze et al. 1986, Lominadze et al.(1986)) and summarized in Paper I. It is worthwhile to recapitulate these arguments here. The emission of waves (by means of curvature radiation) with frequency close to the local plasma frequency  $\omega_{cr} = \omega_o$  is impossible, because one cannot fulfill the following two conditions simultaneously: (1) the timescale of the radiative process must be significantly shorter than the plasma oscillation periods, which means  $\omega_{cr} \gg \omega_o$ , and (2) the linear characteristic dimension of the bunches must be shorter than the wavelength of the radiated wave, which means  $k_{cr} \ll k_o = \omega_o/c$ . On the other hand  $\omega_o = k_o c$  and  $\omega_{cr} = k_{cr} c$ . Thus it is impossible to satisfy the above two conditions simultaneously and therefore bunching associated with high-frequency Langmuir plasma wave cannot be responsible for the coherent pulsar radio-emission (see also Melrose & Gedalin (1999)).

In the soliton model of coherent curvature radiation considered in this paper, the soliton-like bunches are formed due to the non-linear evolution of Langmuir wave packets and thus the sizes of the bunches are naturally much larger than the Langmuir wave-length. Hence the condition  $k_{cr}^{(sol)} \ll k_o$  is always fulfilled (here the superscript “sol” corresponds to soliton.) At the same time the soliton lifetime must be much longer than the period of Langmuir waves ( $\Delta t \gg 2\pi/\omega_o$ ). However,  $\omega_{cr}^{(sol)} \lesssim \Delta t/2\pi$  or  $\omega_{cr}^{(sol)} \ll \omega_o$ . As we have shown, this condition implies that the AWC cannot be satisfied for the plasma modes excited by the soliton curvature radiation mechanism. Thus, the excited plasma waves can retain their initial polarization, while they propagate through the magnetospheric plasma.

### 3.5. O-mode properties

The group velocity of plasma waves describes the velocity and the direction of energy transfer and is defined as

$$\mathbf{v}_g = \mathbf{i} \frac{\partial \omega}{\partial k_{\parallel}} + \mathbf{j} \frac{\partial \omega}{\partial k_{\perp}}. \quad (20)$$

Here  $\mathbf{i}$  and  $\mathbf{j}$  are unit vectors directed along and across the external magnetic field vector. As the dispersion law of X-mode is  $\omega = kc$ , the group and phase velocities of X-mode are equal to each other, thus  $v_g = c$  and  $\mathbf{v}_g \parallel \mathbf{k}$ .

The dispersion law of O-mode can be expressed as  $\omega = k_{\parallel}c(1 - k_{\perp}^2 c^2 / 2\omega_0^2)$ , thus the group velocity of O-mode can be calculated as

$$\mathbf{v}_g = \mathbf{i}c \left( 1 - \frac{k_{\perp}^2 c^2}{2\omega_0^2} \right) - \mathbf{j} \frac{k_{\parallel} k_{\perp} c^3}{2\omega_0^2}. \quad (21)$$

Taking into account that both  $k_{\parallel}$  and  $k_{\perp}$  are much less than  $\omega_0/c$ , it is straightforward to obtain  $\mathbf{v}_g \approx \mathbf{i}c$ . Thus the group velocity of O-mode is directed along the external magnetic field i.e. the O-mode is ducted along  $\mathbf{B}$  preserving direction of the wave vector and eventually decays as a result of the Landau damping (Arons & Barnard 1986). Thus under normal conditions the O-mode cannot escape from the magnetosphere.

Let us consider under what special conditions a fraction of the generated O-mode could escape and reach the observer. Such a possibility can be illustrated by means of schematic Figure 3 presenting wave modes in strongly magnetized plasma. As it has been already stated in Section 2, solution of Equation (8) corresponds to two types of waves: superluminal (L-mode) and subluminal (O-mode). In the case of oblique (nonzero  $\vartheta$ ) propagation both of them are mixed transverse-longitudinal waves (see, e.g. Arons & Barnard 1986, KMM91). Which of those two feature actually dominates depends on the value of ratio  $E_1/E_3$  (recall that  $E_3$  is along  $\mathbf{k}$  and  $E_1$  is in the plane of  $\mathbf{k}$  and  $\mathbf{B}$ ). If  $E_1/E_3 \gg 1$  then the O-mode (polarized in the  $yz$  plane) is mostly transverse and thus almost electromagnetic in nature. In the opposite case if  $E_1/E_3 \ll 1$  the waves are longitudinal plasma oscillations, thus they are non-electromagnetic in nature. Therefore, if one can demonstrate that  $E_1/E_3 \gg 1$  in the radio-emission region then the L-mode (provided it can be excited by some physical mechanism<sup>10</sup>; some possibility will be discussed later) can escape as the observed orthogonal mode with the electric field lying in the plane of curved magnetic field lines.

---

<sup>10</sup>It worth mentioning that the L-mode cannot be excited directly by curvature radiation as it is suppressed by Razin's effect (see Paper II).



Let us now estimate the value of  $E_1/E_3$  within our scenario. It follows from Equation (2)

$$\frac{E_1}{E_3} = \frac{\epsilon_{31}}{k^2 c^2 / \omega^2 - \epsilon_{11}} = \frac{I \sin \vartheta \cos \vartheta}{I \sin^2 \vartheta - (1 - k^2 c^2 / \omega^2)}. \quad (22)$$

Substituting  $I$  from Equation (8), Equation (22) becomes

$$\frac{E_1}{E_3} = - \left( \frac{\omega^2}{k^2 c^2} \right) \frac{\sin \vartheta}{\left( \frac{\omega^2}{k^2 c^2} - 1 \right) \cos \vartheta}. \quad (23)$$

For the superluminal L-mode  $\omega > kc$  and under small  $\vartheta$  approximation (remembering that  $\vartheta \gamma_s > 1$ ) the solution of Equation (8) is

$$\frac{\omega}{kc} = 1 + \frac{1}{2} \frac{1}{\vartheta^2 \gamma_s^4} \left( \frac{\omega_o^2}{k^2 c^2} \right), \quad (24)$$

which is valid provided that

$$\frac{1}{\vartheta^2 \gamma_s^4} \left( \frac{\omega_o^2}{k^2 c^2} \right) \ll 1. \quad (25)$$

Incorporating Equation (24) into Equation (23) we obtain

$$\frac{E_1}{E_3} = \frac{k^2 c^2}{\omega_o^2} 2\vartheta^3 \gamma_s^4 \gg 1. \quad (26)$$

As it has been mentioned earlier, this condition means that the L-mode is almost electromagnetic in nature.

Below we describe a possible scenario how this electromagnetic L-mode can be excited. The shaded region in Figure 3 represents the frequency range of generated waves by means of soliton coherent curvature radiation. Let us recall that our pulsar model is conditional on a non-stationary sparking discharge of the inner accelerating region (PSG). Therefore the resultant secondary plasma must be inhomogeneous in space. In such plasma there should be many regions with steep density gradients along as well as across the magnetic field lines. If the O-mode reaches the steep gradient of plasma density, where the number density (and hence the characteristic frequency  $\omega_o$ ) changes rapidly, then the L-mode curve moves towards the shaded region (shown schematically in Figure 3). Under such condition the O-mode can be linearly coupled with the L-mode and escape as electromagnetic waves (e.g. Arons & Barnard 1986; KMM91). The L-mode also preserves the polarization properties of the ordinary modes since both the L- and O-modes should be linearly polarized in the same plane, which is orthogonal to the polarization plane of X-mode. Thus the observed secondary polarization mode (i.e. the ordinary mode) will be polarized in the plane of curved magnetic field lines. It is worth realizing that most of the generated power is contained in the O-mode

(about 6 times stronger than the X-mode; see footnote 2). Therefore, only small fraction of this mode has to escape to explain the observed level of the weaker secondary polarization mode.

Finally, it is important to emphasize that the escape of L-mode should happen before the O-mode is damped. This problem however is beyond the scope of discussion of this work, and will be addressed in a forthcoming paper.

#### 4. Conclusions

In this paper we have shown the observational evidences that the linearly polarized waves emerge from the magnetosphere either parallel or perpendicular to the magnetic field line planes. We associate these waves with the X- and O-modes excited by soliton coherent curvature radiation in the secondary plasma. The above conclusion is true if the waves emerge from the magnetosphere as they are generated, preserving their polarization properties. In other words the AWC should not hold in the pulsar magnetosphere within the soliton coherent curvature radiation model.

We have demonstrated that properties of the pulsar plasma as well as features of the soliton coherent curvature radiation emission mechanism provide the proper conditions for the generation of pulsar radio emission at the altitudes well below 10% of the light cylinder radius (see Figure 4 and section 3.2 and 3.3), which is in a good agreement with observations. Then in section 3.4 we proceeded to show that in this emission region the difference between the refractive indexes of O- and X-modes  $N = N^o - N^x$  is negligibly small (see Figure 5) for the frequency range  $\omega \ll \omega_o$ , for which the soliton coherent curvature radiation can operate. This implies that  $N \sim 0$  and hence the AWC given by Equation (14) cannot be satisfied. It is important to note that our conclusion differs from that of CR79 since they calculated the AWC condition at  $\omega \sim \omega_o$ , while for our case  $\omega \ll \omega_o$ . The excited waves can hence retain their initial polarization as they propagate in the magnetospheric plasma. The X-mode, which is electromagnetic in nature, escapes from the pulsar magnetosphere and represents the PPM highly polarized subpulses showcased by Paper III. Although observationally there exist highly polarized pulses in the SPM, they cannot be related directly to the O-mode, as under normal circumstances this mode gets damped and cannot escape. As a possible interpretation of the SPM we suggest in Section 3.5 that if there are steep density gradients in the radiation excitation region, then the O-mode couples to the L-mode and can emerge as the secondary polarization mode polarized in the planes of the curved magnetic field lines.

We thank the anonymous referee for his critical comments which helped us to improve

the manuscript significantly. This paper was financed by the Grant DEC-2012/05/B/ST9/03924 of the Polish National Science Center. JG and GM are grateful to the Inter University Centre for Astronomy and Astrophysics, Pune India, for their kind hospitality during their stay there where the important part of this work was completed. We thank Dipankar Bhattacharya for giving extensive support during this work. We thank Rahul Basu for critical reading of the manuscript and comments. This paper used data from the Giant Meterwave Radio Telescope, and we thank the staff of the GMRT for their technical support provided during these observations. GMRT is run by the National Centre for Radio Astrophysics of the Tata Institute of Fundamental Research

## REFERENCES

- Arons, J. & Barnard, J. J., 1986, *ApJ*, 302, 120
- Asseo, E., & Melikidze, G. I., 1998, *MNRAS*, 301, 59
- Blaskiewicz, M., Cordes, J. M., & Wasserman, I., 1991, *ApJ*, 370, 643
- Benford, G. & Buschauer, R., 1983, *A&A*, 118, 358
- Cordes, J. M., 1978, *ApJ*, 222, 1006.
- Cowsik, R., 1998, *A&A*, 340, L65
- Cheng, A. F. & Ruderman, M. A., 1979, *ApJ*, 229, 348
- Gangadhara, R. T. & Gupta, Y., 2001, *ApJ*, 555, 31
- Geppert, U., Gil, J. & Melikidze, G., 2013, *MNRAS*, 435, 3262
- Gil, J., Melikidze, G. I. & Geppert, U., 2003, *A&A*, 407, 315
- Gil, J., Lyubarsky, Y., & Melikidze, G. I., 2004, *ApJ*, 600,872 (Paper II)
- Ginzburg, V. L. & Zhelezniakov, V. V., 1979, *ARA&A*, 13, 511
- Jackson, J.D., 1975, *Classical Electrodynamics*, New York: Wiley)
- Johnston, S., Hobbs, G., Vigeland, S., Kramer, M., Weisberg, J. M., & Lyne, A. G., 2005, *MNRAS*, 364, 1397
- Jones, P. B., 1986, *MNRAS*, 218, 477

- Kazbegi, A. Z., Machabeli, G. Z. & Melikidze, G. I., 1991, MNRAS, 253, 377 (KMM91)
- Kijak, J. & Gil, J., 1997, MNRAS, 288, 631
- Krzyszowski, K., Mitra, D., Gupta, Y. & Kijak, J., Gil, J. & Acharyya, A., 2009, MNRAS, 393, 1617.
- Lai, D., Chernoff, D. F., & Cordes, J. M., 2001, ApJ, 549, 1111
- Lominadze, J. G., Machabeli, G. Z., Melikidze, G. I., & Pataraya, A. D., 1986, Sov. J. Plasma Phys., 12, 712
- Melikidze, G. I, Gil, J., & Pataraya, A. D. 2000, ApJ, 544, 1081 (Paper I)
- Melikidze, G. I., & Pataraya, A. D., 1980, Astrophysics, 16, 161
- Melikidze, G. I., & Pataraya, A. D., 1984, Astrophysics, 20, 157
- Melrose, D. B., & Gedalin, M. E., 1999, ApJ, 521, 351
- Medin, Z. & Lai, D., 2006, Phys. Rev. A, 74, 062507
- Medin, Z. & Lai, D., 2007, MNRAS, 382, 1833
- Mitra, D & Deshpande, A. A., 1999, A&A346, 906
- Mitra, D., Gil, J. & Melikidze, G. I., 2009, ApJ, 696L, 141 (Paper III)
- Mitra, D. & Li, X. H., 2004, A&A, 421, 215
- Mitra, D, Rankin, J. M. & Gupta, Y., 2007, MNRAS, 379, 932
- Morris, D., Graham, D. A., Sieber, W., Jones, B. B., Seiradakis, J. H. & Thomasson, P., 1979, A&A, 73, 46.
- Morris, D., Graham, D. A., Sieber, W., Bartel, N. & Thomasson, P., 1981, A&AS, 46, 121
- Noutsos, A., Kramer, M., Carr, P. & Johnston, S., 2012, MNRAS, 423, 2736.
- Noutsos, A., Schnitzeler, D. H. F. M., Keane, E. F., Kramer, M. & Johnston, S., 2013, MNRAS, 430, 2281.
- Pataraya, A. & Melikidze, G., 1980, Ap&SS, 68, 49
- Rankin, J. M., 1993, ApJ, 405, 285

- Rankin, J. M., 2007, *ApJ*, 664, 443
- Spruit, H. & Phinney, E. S., 1998, *Nature*, 393, 139
- Szary, A., 2013, PhD thesis, arXiv:1304.4203
- Tademaru E. & Harrison E. R., 1975, *Nature*, 254, 676
- Radhakrishnan V., & Cooke D. J., 1969, *ApJ*, 3, 225
- Ruderman, M. A., & Sutherland, P. G., 1975, *ApJ*, 196, 51
- Usov, V. V., 1987, *ApJ*, 320, 333

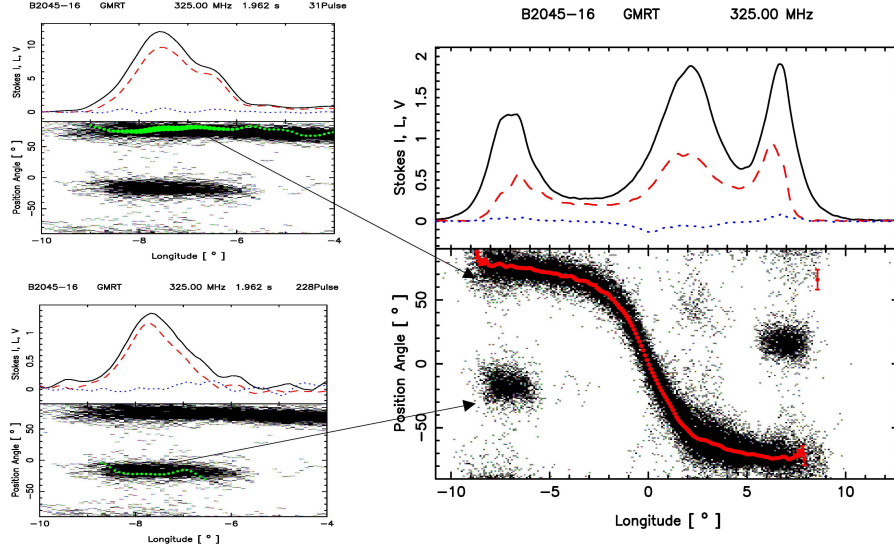


Fig. 1.— The right hand figure in this plot shows the average pulse profile of PSR B2045–16. The top panel of this plot shows the total intensity in black, linear polarization in dashed red lines and circular polarization in dotted blue lines. In the bottom panel the red curve is the average PPA track computed using the average Stokes  $U$  and  $Q$ , and the dotted points are the PPA histograms which are obtained by overplotting the PPA of every single pulse. The average PPA follow the more frequently occurring PPA track known as the primary polarization mode (PPM) and the other one is called the secondary polarization mode (SPM). The two plots in the left hand panel show two highly polarized subpulses occurring close to the leading profile component. The top subpulse is dominated by PPM and the bottom one is dominated by the SPM. In these subpulses the corresponding PPA are displayed in green, overlaid on the same dotted histograms as displayed in the right panel for easy reference. These histograms are exactly the same in all the panels of Figures 1 and 2, as they represent all position angle data taken for this pulsar. It is important to realize that these two subpulses are by no means exceptional. An exemplary collection of similar cases can be viewed in Figure 2

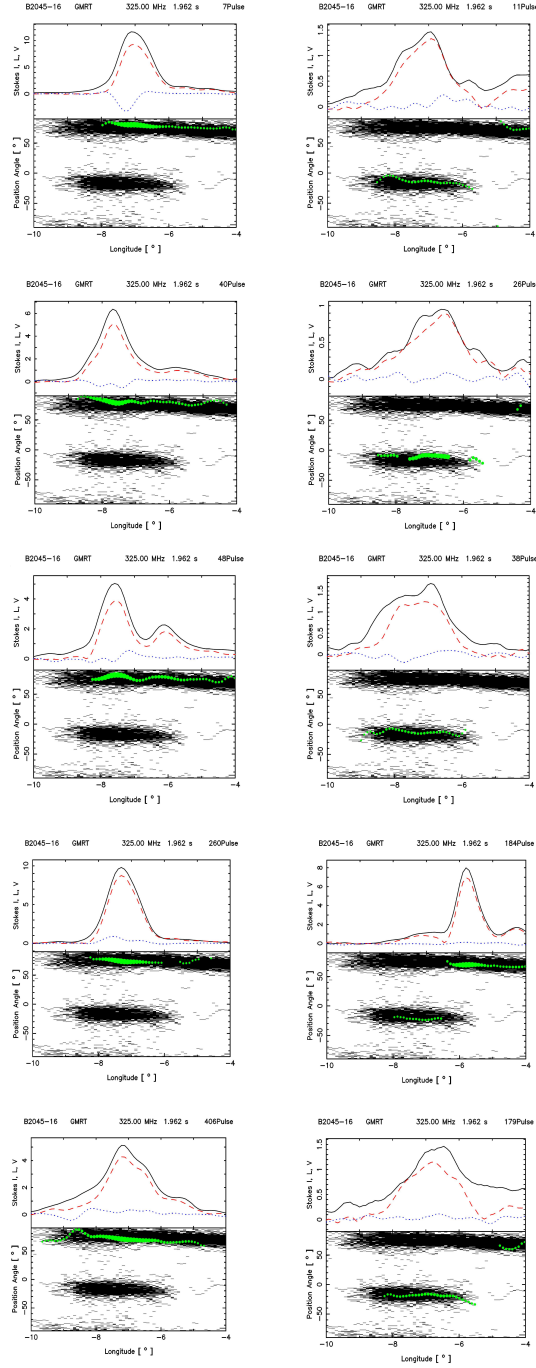


Fig. 2.— This Figure shows 5 more examples of highly polarized subpulses shown the same way as in Figure 1. The left panels show stronger subpulses dominated by the primary polarization mode (PPM). The right panels show weaker subpulses dominated by the secondary polarization mode (SPM). However, in these panels there are also subpulses dominated by PPM, although in all presented individual pulses the single subpulses are always polarized in one of the modes. For further details see section 2.

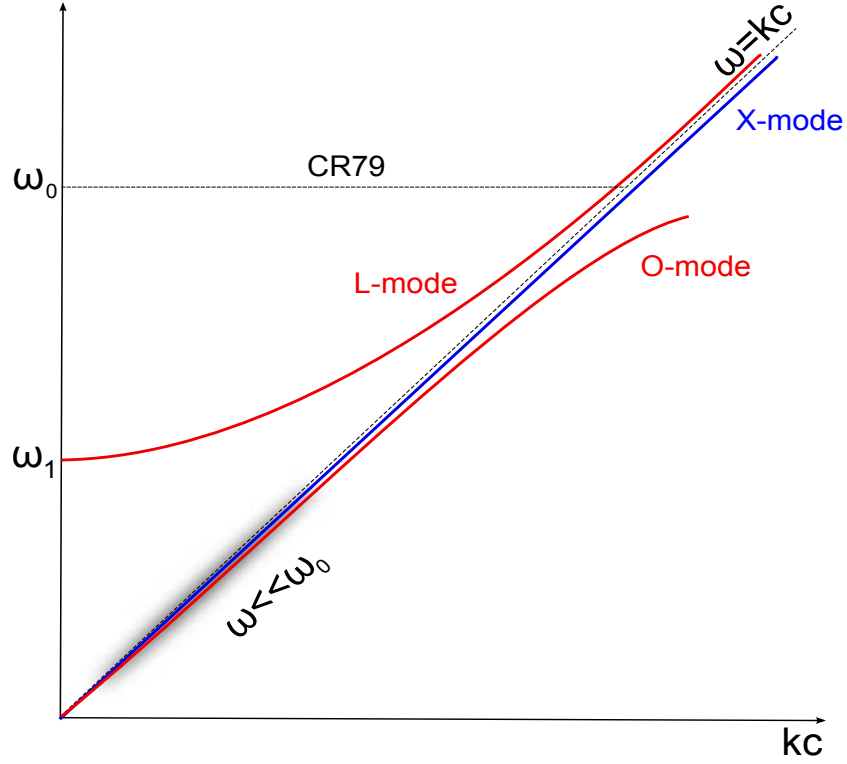


Fig. 3.— Schematic representation of the electron positron plasma eigen-modes in infinitely strong magnetic field in the case of oblique ( $\vartheta \neq 0$ ) propagation. The shadowed region represents the frequency range  $\omega \ll \omega_0$  characteristic for the soliton curvature radiation, while the level  $\omega > \omega_0$  corresponds to the linear Langmuir oscillations used by CR79, which, however, cannot emit any coherent curvature radiation. In the case of parallel propagation ( $\vartheta = 0$ ) the O-mode coincides with the X-mode, while the L-mode becomes a strictly longitudinal Langmuir wave. The dispersion curve of the Langmuir waves crosses the  $\omega = kc$  line at the point  $\omega = \omega_0$ .



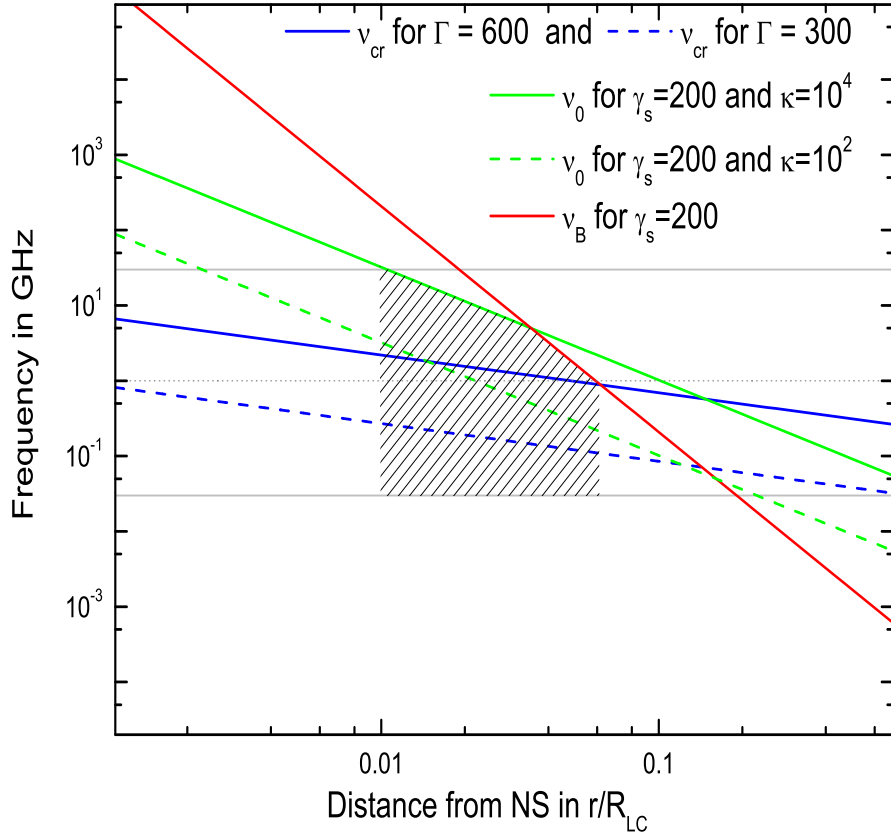


Fig. 4.— Basic plasma parameters in the observers frame of reference for a typical pulsar with period  $P = 1$  sec and  $\dot{P} = 10^{-15}$ . See legend in the figure and the text in Section 3.2 for details. The abscissa originates at about 50 km altitude ( $r/R_{LC} \sim 10^{-3}$ ), below which the two stream instability is not able to develop. The dashed area represents (from a purely theoretical point of view) the most likely region of generation of the observed pulsar radio emission.

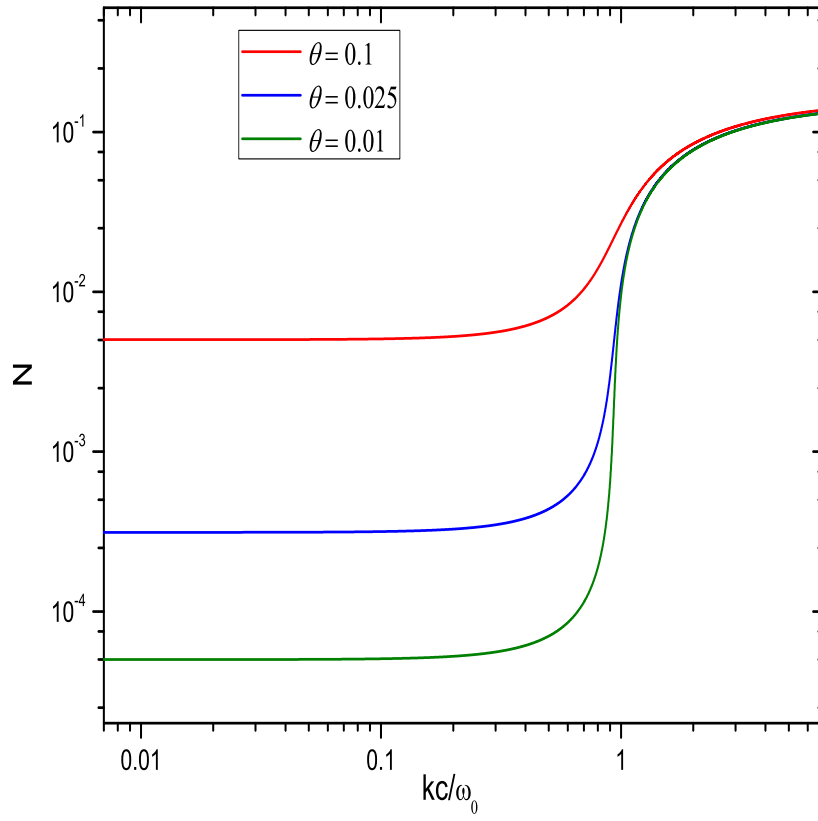


Fig. 5.— The plot shows the numerical solutions of Equation (8) for three values of  $\vartheta$ .